Development 140, 1936-1945 (2013) doi:10.1242/dev.087718

Zebrafish Foxi1 provides a neuronal ground state during inner ear induction preceding the Dlx3b/4b-regulated sensory lineage

Stefan Hans*, Anne Irmscher and Michael Brand*

SUMMARY

Vertebrate inner ear development is a complex process that involves the induction of a common territory for otic and epibranchial precursors and their subsequent segregation into otic and epibranchial cell fates. In zebrafish, the otic-epibranchial progenitor domain (OEPD) is induced by Fgf signaling in a Foxi1- and Dlx3b/4b-dependent manner, but the functional differences of Foxi1 and Dlx3b/4b in subsequent cell fate specifications within the developing inner ear are poorly understood. Based on pioneer tracking (PioTrack), a novel Cre-dependent genetic lineage tracing method, and genetic data, we show that the competence to embark on a neuronal or sensory fate is provided sequentially and very early during otic placode induction. Loss of Foxi1 prevents neuronal precursor formation without affecting hair cell specification, whereas loss of Dlx3b/4b inhibits hair cell but not neuronal precursor formation. Consistently, in Dlx3b/4b- and Sox9a-deficient *b380* mutants almost all otic epithelial fates are absent, including sensory hair cells, and the remaining otic cells adopt a neuronal fate. Furthermore, the progenitors of the anterior lateral line ganglia also arise from the OEPD in a Foxi1-dependent manner but are unaffected in the absence of Dlx3b/4b or in *b380* mutants. Thus, in addition to otic fate Foxi1 provides neuronal competence during OEPD induction prior to and independently of the Dlx3b/4b-mediated sensory fate of the developing inner ear.

KEY WORDS: Inner ear, Neurogenesis, Competence, Foxi1, Dlx3b/4b, Genetic lineage tracing, Cre/lox, PioTrack, Zebrafish

INTRODUCTION

The vertebrate inner ear mediates hearing and balance through a complex arrangement of mechanosensory hair cells, nonsensory supporting cells and sensory neurons. All of these cell types derive from the otic placode, a transient ectodermal thickening adjacent to the developing hindbrain (Barald and Kelley, 2004; Fritzsch et al., 2006). Otic placode formation is a multistep process initiated by the establishment of the preplacodal region, which surrounds the anterior neural plate and contains precursors for all sensory placodes (Streit, 2007). Subsequently, the otic-epibranchial progenitor domain (OEPD), a common territory for otic and epibranchial precursors, is specified (Ladher et al., 2010; Chen and Streit, 2012). In zebrafish, the OEPD also appears to contain the progenitors of the anterior lateral line ganglion (McCarroll et al., 2012). Studies in various species have shown that OEPD formation is triggered by Fibroblast growth factor (Fgf) ligands secreted by the hindbrain and subjacent mesendoderm (Phillips et al., 2001; Léger and Brand, 2002; Maroon et al., 2002; Alvarez et al., 2003; Wright and Mansour, 2003; Ladher et al., 2005). In response to these signals, cells express Pax8 and Pax2, two members of the Pax2/5/8 transcription factor family, which are crucial regulators of OEPD formation and proper inner ear development (Brand et al., 1996; Pfeffer et al., 1998; Hans et al., 2004; Mackereth et al., 2005; Bouchard et al., 2010; Freter et al., 2012). The subsequent segregation of otic and epibranchial progenitors is mediated by Wnt signaling in a Pax2-dependent manner (Freter et al., 2008; McCarroll et al., 2012). With respect to otic fate, a two-phase model has been proposed to summarize genetic interactions during otic induction in zebrafish (Hans et al., 2004; Solomon et al., 2004). According to this model, the forkhead transcription factor Foxi1 enables expression of Pax8 during the early phase, and the homeodomain transcription factors Dlx3b and Dlx4b (Dlx3b/4b) provide competence to activate Pax2a during the second phase (Hans et al., 2004; Solomon et al., 2004). Previous work has shown that *dlx3b*, *dlx4b* and *foxi1* are regulated initially independently in a BMP-dependent manner in the same region at late gastrula stages and whereas *foxi1* is progressively restricted to the presumptive OEPD, *dlx3b* and *dlx4b* are maintained in a stripe corresponding to cells of the preplacodal region (Akimenko et al., 1994; Ellies et al., 1997; Nissen et al., 2003; Solomon et al., 2003; Solomon et al., 2004; Hans et al., 2007). Subsequently, downregulation of *foxi1* in a Pax2a- and Pax8-dependent manner is required for proper otic development, whereas *dlx3b* and *dlx4b* are maintained in the cells of the future otic placode (Akimenko et al., 1994; Padanad and Riley, 2011). Loss of Foxi1 or Dlx3b/4b results in compromised otic induction and development of smaller otic vesicles (Solomon and Fritz, 2002; Liu et al., 2003; Nissen et al., 2003; Solomon et al., 2003), and combined loss of both factors eliminates all indications of otic specification (Hans et al., 2004; Solomon et al., 2004). However, the functional differences of Foxi1 and Dlx3b/4b during otic induction have not been addressed thus far and remain elusive.

After placode formation, otic tissue develops into the otic vesicle where sensory neurons and mechanosensory hair cells are born. The neuronal precursors delaminate as neuroblasts from an anterior-ventral position in the otic vesicle and give rise to the eighth cranial or statoacoustic ganglion, whereas hair cells are generated in the sensory epithelia of the otic vesicle (Haddon and Lewis, 1996;

Technische Universität Dresden, Biotechnology Center and DFG-Center for Regenerative Therapies Dresden Cluster of Excellence, Tatzberg 47-49, 01307 Dresden, Germany.

*Authors for correspondence (stefan.hans@biotec.tu-dresden.de; michael.brand@biotec.tu-dresden.de)

Accepted 11 February 2013

Rubel and Fritzsch, 2002). It is well established that neuroblast and hair cell formation require the activation of the proneural proteins Neurogenin 1 (Neurog1) and Atonal homolog 1 (Atoh1) (Ma et al., 1998; Bermingham et al., 1999; Andermann et al., 2002; Fritzsch et al., 2010). However, despite an understanding of proneural gene function and extensive research on otic placode induction, upstream events, including the underlying regulation of Atoh1 and Neurog1 expression in sensory and neuronal precursors, are just beginning to be understood. In zebrafish, it was shown that Dlx3b/4b is required for proper expression of *atoh1a* and *atoh1b* and subsequent formation of mechanosensory hair cells (Millimaki et al., 2007). However, clonal analyses have indicated only a limited relationship between neurons and hair cells with regional differences within the developing inner ear (Satoh and Fekete, 2005; Abello and Alsina, 2007; Sapède et al., 2012). Currently, it is unknown whether lineage commitment followed by proneural activation of Neurog1 and Atoh1 occurs in separate neuronal and sensory domains, or in a common neurogenic domain.

Here, we demonstrate that the competence to enter a neuronal or sensory fate is provided sequentially by Foxi1 and Dlx3b/4b very early during inner ear development. Initially, Foxi1, a known otic competence factor, induces the OEPD and provides competence to enter a neuronal fate. Consequently, inactivation of Foxi1 does not only result in compromised otic vesicle formation, but in a loss of all neuronal OEPD derivatives, including the statoacoustic, anterior lateral line and epibranchial ganglia, which has been reported previously (Lee et al., 2003), Subsequently, Dlx3b/4b, which is able to provide otic fate in the absence of Foxi1, restricts neuronal and promotes sensory fate.

MATERIALS AND METHODS

All animal experiments were conducted according to the guidelines and under supervision of the Regierungspräsidium Dresden (permit AZ 24D-9168.11-1/2008-1 and AZ 24D-9168.11-1/2008-4). All efforts were made to minimize animal suffering and the number of animals used.

Zebrafish husbandry and germline transformation

Zebrafish were raised and maintained as described previously (Brand et al., 2002). Zebrafish embryos were obtained by natural spawning of adult fish and staged according to hours post-fertilization (hpf) or standard criteria (Kimmel et al., 1995). The wild-type line used was AB. The conditional red-to-green reporter *Tg(hsp70l:loxP-DsRed-loxP-EGFP)*, the DsRed gene trap into the *pax8* locus in $pax8^{nia03Gt}$, the null allele $foxi1^{em1}$ and the deletion of *dlx3b*, *dlx4b* and *sox9a* in Df^{b380} have been described previously (Fritz et al., 1996; Solomon et al., 2003; Ikenaga et al., 2011; Kroehne et al., 2011). For germ-line transformation, the pTol $pax2a:CreER^{T2}$ plasmid was injected into fertilized eggs, embryos were raised to adulthood and crossed to AB wild-type fish, and the resulting F1 embryos were screened by PCR as previously described (Hans et al., 2009).

Immunocytochemistry and *in situ* hybridization

Antibodies used were anti-GFP (Molecular Probes; 1:500) and peroxidase-conjugated goat anti-rabbit IgG (whole molecule) (Sigma: A0545; 1:500). cDNA probes that detect the following genes were used: *neurog1* and *neurod* (Andermann et al., 2002); *stm* (Söllner et al., 2003); *cdh6* and *cdh10* (Liu et al., 2006); *myo7aa* (Ernest et al., 2000); *atoh1b* (Adolf et al., 2004); *tbx1* (Piotrowski et al., 2003); *pax2a* (Krauss et al., 1991); *phox2a* and *phox2bb* (Guo et al., 1999); *tlx3b* (Langenau et al., 2002); and $CreER^{T2}$ (Hans et al., 2009). Antibody staining, probe synthesis and *in situ* hybridization were performed as previously described (Westerfield, 2000).

Morpholinos, pharmacological and heat treatments

Morpholino oligomers (MOs) were obtained from Gene Tools. MOs for *neurog1* and *foxi1* were described previously (Andermann et al., 2002; Solomon et al., 2003). For tamoxifen (Sigma, T5648) treatment a 50 mM stock solution in DMSO was made and stored at −20°C. At early gastrulation stages (6 hpf), embryos, still in their chorions, were transferred into Petri dishes containing 0.5 μM tamoxifen solution and incubated in the dark until heat treatments were conducted at the indicated stages. For subsequent heat-shock treatment, embryos were transferred into fresh Petri dishes. After removal of excess embryo medium, 42°C embryo medium was added, incubated for 0.5 hours at 37°C, returned to 28.5°C and fixed at 24 hpf.

RESULTS

Early *pax2a*-positive OEPD cells give rise to delaminated neuroblasts and the anterior-ventral part of the otic vesicle

Previous fate-mapping experiments using Kaede and caged fluorescein-dextran have shown that the Pax2-positive OEPD contributes to the otic vesicle, the epibranchial and presumably the anterior lateral line ganglia (McCarroll et al., 2012). Similarly, genetic lineage tracing in mice using the Cre/loxP recombination system revealed that OEPD Pax2-expressing cells give rise to the otic placode, as well as to epidermis (Ohyama and Groves, 2004b). Recently, we showed that Cre/loxP is also highly efficient in zebrafish (Hans et al., 2009; Hans et al., 2011; Kroehne et al., 2011). In common genetic lineage-tracing analyses, reporter expression is usually driven by a constitutive promoter and directly linked to Cre-mediated recombination. Consequently, all Cre-positive cells activate the reporter and indicate the cell fates of the entire Cre domain at later stages (Fig. 1A,B). By contrast, we devised a novel Cre-mediated lineage-tracing method called pioneer tracking (PioTrack) that allows fate mapping specifically of the first Cre-expressing cells of a nascent Cre domain, if the domain subsequently expands by *de novo* Cre expression in neighboring cells. PioTrack employs a conditional promoter, which can disconnect Cre-mediated recombination from reporter activation. We used the zebrafish temperature-inducible *hsp70l* promoter, which is expressed strongly and ubiquitously only during heat treatment (Halloran et al., 2000). Application of heat during the early stages of a nascent Cre domain results in reporter expression in only those cells that have undergone recombination, and persistence of the reporter protein reveals the fates of these cells at later stages (Fig. 1C). Application of heat at later stages, after Cre is expressed throughout the entire domain, activates reporter expression and indicates cell fates of the entire Cre domain in a manner similar to common genetic lineage tracing (Fig. 1D). To use PioTrack in early otic development, we generated the transgenic line $Tg(pax2a:CreER^{T2})^{\#31}$ driving $CreER^{T2}$ in the OEPD, using a *pax2a* promoter fragment that faithfully recapitulates OEPD expression and has been used in previous studies (Picker et al., 2002; Hans et al., 2009; McCarroll et al., 2012). To confirm the utility of $Tg(pax2a:CreER^{T2})^{\#31}$, we performed *in situ* hybridizations with *pax2a* and $CreER^{T2}$ probes (supplementary material Fig. S1). Compared with *pax2a*, $CreER^{T2}$ is absent in the midbrain-hindbrain boundary and ectopic expression is found in rhombomeres 3 and 5 during early segmentation stages as previously reported (Picker et al., 2002; Hans et al., 2009). By contrast, $CreER^{T2}$ expression in the OEPD closely recapitulates the endogenous *pax2a* expression in a temporal and spatial manner (supplementary material Fig. S1A-D,F-I) as confirmed by double color *in situ* hybridization (Fig. 1E-G′). Only after otic placode formation does *pax2a* and $CreER^{T2}$ expression diverge when $CreER^{T2}$ is not downregulated in $Tg(pax2a:CreER^{T2})^{\#31}$ anteriorly to the otic placode (supplementary material Fig. S1E,J). We crossed $Tg(pax2a:CreER^{T2})^{\#31}$ with the conditional red-to-green reporter *Tg(hsp70l:loxP-DsRed-loxP-EGFP)* (Kroehne et al., 2011), applied tamoxifen to elicit immediate Cre-mediated recombination as soon

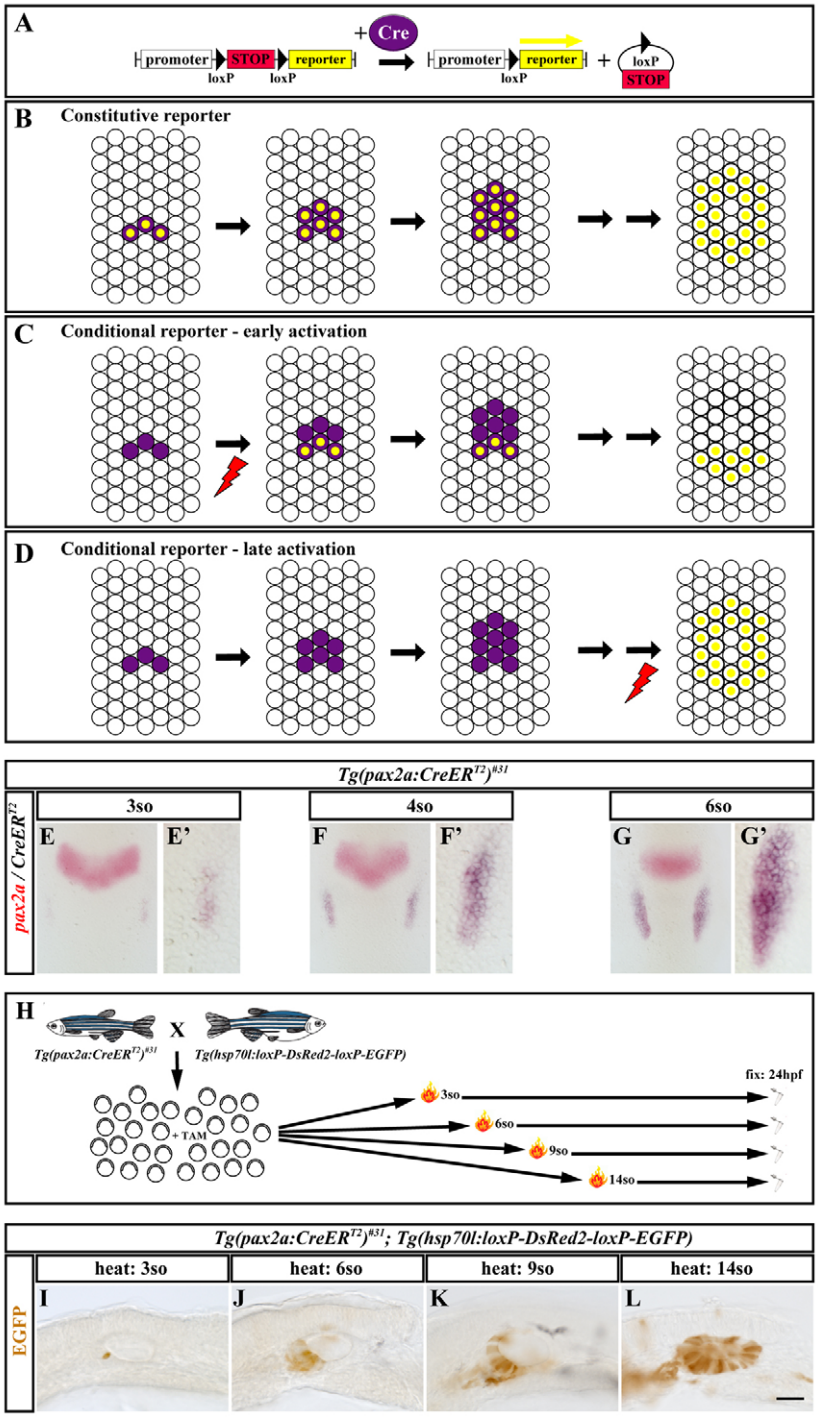

Fig. 1. Pioneer tracking reveals that early OEPD *pax2a*-positive cells predominantly contribute to the anterior-ventral part of the otic vesicle, including the neurogenic region. (**A**) Removal of a loxP-flanked transcriptional STOP cassette (red) in the presence of Cre (purple) activates reporter expression (yellow). (**B**) In a common genetic lineage-tracing setup, Cre expression and reporter activation are directly linked by the constitutive promoter driving reporter expression. Consequently, the reporter is active in all Cre-positive cells even at later stages when Cre expression has vanished. (**C**) By contrast, use of the conditional temperature-inducible *hsp70l* promoter uncouples Cre expression and reporter activation. Early activation (red thunderbolt) restricts reporter expression to cells that experience recombination within a nascent Cre domain and allows fate mapping of these cells due to reporter protein persistence at later stages. (**D**) Late activation (red thunderbolt) of the conditional promoter reveals the fate of the entire Cre domain at later stages similar to a constitutive promoter. (**E-G**) *CreER*^{T2} (blue) recapitulates the dynamic, endogenous *pax2a* expression (red) during OEPD stages (3-, 4-, 6-somite) in transgenic *Tg(pax2a:CreER*^{T2}*)*$^{\#31}$ embryos shown by two-color *in situ* hybridization. (**E′-G′**) High magnification views of the OEPD region of embryos shown in E-G, respectively. (**H**) Schematic of the experimental outline. The progeny of the indicated cross were exposed to tamoxifen (TAM) to elicit immediate Cre-mediated recombination as soon as *CreER*^{T2} is active. Subsequently, the offspring were divided into different groups, exposed to a single heat treatment at various developmental stages [3-, 6-, 9-, 14-somites (so)] and analyzed at 24 hpf. (**I**,**J**) EGFP-labeled cells are found in an anterior-ventral position within the otic vesicle after heat shock at the 3- or the 6-somite stage in *Tg(pax2a:CreER*^{T2}*)*$^{\#31}$*; Tg(hsp70l:loxP-DsRed-loxP-EGFP)* double transgenic embryos. (**K**) Heat shock at the 9-somite stage expands the EGFP-positive domain without labeling posterior-dorsal positions within the otic vesicle. (**L**) EGFP-labeled cells can be detected throughout the otic vesicle after heat shock at placodal stages. E-G are dorsal views with anterior to the top at 3-, 4-, 5- and 12-somite stages. I-L are lateral views with anterior to the left at 24 hpf. Scale bars: in L, 90 μm for E-G; in L, 30 μm for E′-G′; in L, 40 μm for I-L.

as *CreER*^{T2} is expressed, divided the embryos into different groups and provided heat treatments at various developmental stages (Fig. 1H). Using this strategy, we find that enhanced green fluorescent protein (EGFP)-labeled cells end up as delaminated neuroblasts and in an anterior-ventral position within the otic vesicle after heat treatments at early OEPD stages, including the 3- and the 6-somite stages (Fig. 1I,J). Heat treatments at late OEPD stages, including the 9-somite stage, enlarge the domain, but no labeled cells populate the posterior-dorsal region (Fig. 1K). By contrast, EGFP-labeled cells are present throughout the otic vesicle after heat treatment at placodal or vesicle stages (Fig. 1L; data not shown). Taken together, our results show that early OEPD *pax2a*-positive cells give rise predominantly to the anterior-ventral part of the otic vesicle, including the neurogenic region, but do not contribute randomly to the entire otic vesicle.

Independent regulation of sensory and neuronal lineages by Dlx3b/4b and Foxi1

The finding that early *pax2a*-positive OEPD cells are spatially restricted within the developing inner ear suggests that neuronal fate might already be specified within the OEPD very early on. In zebrafish, the transcription factors Foxi1 and Dlx3b/4b play pivotal roles during otic induction, and Dlx3b/4b is essential for sensory lineage development (Nissen et al., 2003; Solomon et al., 2003;

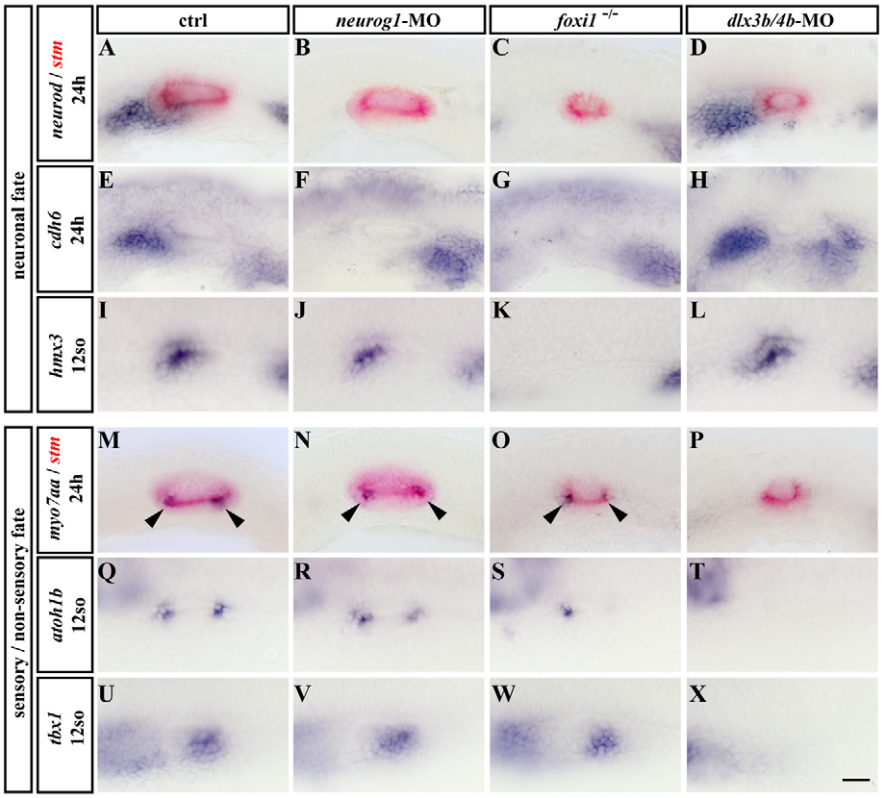

Fig. 2. Foxi1 and Dlx3b/4b regulate the neuronal and sensory lineages of the inner ear. (**A-X**) Blue: Expression of *neurod* (A-D), *cdh6* (E-H), *hmx3* (I-L), *myo7aa* (M-P), *atoh1b* (Q-T) and *tbx1* (U-X) in control (A,E,I,M,Q,U), *neurog1*-MO injected (B,F,J,N,R,V), *foxi1* mutant (C,G,K,O,S,W) and *dlx3b/4b*-MO injected embryos (D,H,L,P,T,X). Red: Expression of *stm* reveals the size of the otic vesicle, which is reduced in *foxi1* mutant and *dlx3b/4b*-MO injected embryos. A-H,M-P are lateral views with anterior to the left at 24 hpf. I-L,Q-X are dorsolateral views with anterior to the left at the 12-somite stage. Arrowheads indicate the position of the sensory patches. Scale bar: 40 μm.

Millimaki et al., 2007). To test whether Dlx3b/4b is also required for the neuronal lineage during otic development, we examined *neurogenic differentiation* (*neurod*) and *cadherin 6* (*cdh6*) expression (Andermann et al., 2002; Liu et al., 2006). In control embryos at 24 hpf, *neurod* is expressed in the anterior-ventral region of the otic vesicle and in delaminated neuroblasts, whereas *cdh6* is expressed in delaminated neuroblasts only (Fig. 2A,E). At this stage, both *neurod* and *cdh6* also label progenitors of the anterior lateral line ganglia (gALL) that are closely associated with the delaminated neuroblasts of the otic vesicle (Andermann et al., 2002; Liu et al., 2006). In the absence of Dlx3b/4b, *neurod* and *cdh6* expression are slightly increased or unaffected (Fig. 2D,H; Table 1), rather than being reduced, despite smaller otic vesicles as indicated by *starmaker* (*stm*) expression, a marker of the entire epithelium of the otic vesicle (Söllner et al., 2003). By contrast, removal of Foxi1 activity (Fig. 2C,G), which also results in smaller otic vesicles, severely reduces or even abolishes expression of both *neurod* and *cdh6* in a manner similar to the removal of Neurog1 (Fig. 2B,F), which is required for the development of all zebrafish cranial ganglia, including the statoacoustic and anterior lateral line ganglia (Andermann et al., 2002). At vesicle stages, *homeo box (H6 family) 3* (*hmx3*) is also expressed in delaminated neuroblasts and in an anterior-ventral position of the otic vesicle; however, in contrast to *neurod*, *hmx3* is already initiated in the anterior portion of the developing otic placode by the 12-somite stage (15 hpf), prior to expression of Neurog1 (Adamska et al., 2000). Compared with control embryos, loss of Neurog1 or Dlx3b/4b activity does not affect placodal *hmx3* expression, whereas loss of Foxi1 completely abolishes *hmx3* at placodal stages (Fig. 2I-L). We also readdressed the functions of Foxi1 and Dlx3b/4b in sensory lineage development using *myosin VIIAa* (*myo7aa*), a marker of sensory hair cells (Ernest et al., 2000), and *atonal homolog 1b* (*atoh1b*), a proneural gene required for hair cell formation (Adolf et al., 2004; Millimaki et al., 2007). In 24 hpf control embryos, *myo7aa* is expressed in discrete anterior and posterior domains of the otic vesicle corresponding to the prospective utricular and saccular maculae, which are indicated at the 12-somite stage by *atoh1b* expression (Fig. 2M,Q). Both *myo7aa* and *atoh1b* expression are present in the absence of Neurog1 or Foxi1, which, however, frequently results in the formation of only one sensory patch (Fig. 2N,O,R,S). By contrast, and as previously reported (Millimaki et al., 2007), removal of Dlx3b/4b activity results in the complete loss of *myo7aa* and *atoh1b* (Fig. 2P,T). We also examined *T-box 1* (*tbx1*), which is expressed in the non-neurogenic otic territory during placodal and vesicle stages (Piotrowski et al., 2003; Radosevic et al., 2011). We found that Dlx3b/4b-depleted embryos at the 12-somite stage also show a complete absence of *tbx1* compared with control embryos or embryos lacking Neurog1 or Foxi1 activity (Fig. 2U-X).

The observation that absence of Foxi1 frequently results in smaller otic placodes or vesicles containing only one sensory patch suggested that Foxi1 might regulate hair cell formation, either directly or indirectly, and we thus analyzed sensory lineage development in *foxi1* mutants in more detail. In control siblings, a broad and robust *atoh1b* expression can be detected during early OEPD stages, and over time this single domain resolves into two smaller patches (Millimaki et al., 2007), which give rise to the prospective utricular and saccular maculae (supplementary material Fig. S2A,D,G). By contrast, all *foxi1* mutants show reduced *atoh1b* expression at OEPD stages although the degree of reduction is highly variable (supplementary material Fig. S2B,C). Subsequently, a strong correlation of otic placode or vesicle size with sensory patch number can be observed with small or medium-sized placodes or vesicles displaying one or two sensory patches, respectively (supplementary material Fig. S2E,F,H,I). Thus, the neuronal lineage of the inner ear is regulated by Foxi1. By contrast, the sensory lineage is regulated by Dlx3b/4b and only indirectly by Foxi1;

Table 1. Quantification of expression patterns in wild-type, mutant and morpholino (MO)-injected embryos

		Expression level				
Gene	Genotype	Missing	Reduced	Normal	Increased	Total
neurod (24 hpf)	*foxi1*$^{-/-}$	33	9	0	0	42
	dlx3b/4b-MO	0	0	31	34	65
	b380	0	0	25	12	37
	b380; *neurog1*-MO	18	3	0	0	21
	b380; *foxi1*-MO	16	2	0	0	18
cdh6 (24 hpf)	*foxi1*$^{-/-}$	28	6	0	0	34
	dlx3b/4b-MO	0	0	20	26	46
	b380	0	0	17	8	25
	b380; *neurog1*-MO	17	2	0	0	19
	b380; *foxi1*-MO	16	1	0	0	17
hmx3 (12 so)	*foxi1*$^{-/-}$	22	0	0	0	22
	dlx3b/4b-MO	0	0	0	34	34
	b380	0	3	12	0	15
	b380; *neurog1*-MO	0	1	12	0	13
	b380; *foxi1*-MO	15	2	0	0	17
myo7aa (24 hpf)	*foxi1*$^{-/-}$	0	18*	21	0	39
	dlx3b/4b-MO	48	4	0	0	52
	b380	16	0	0	0	16
atoh1b (12 so)	*foxi1*$^{-/-}$	0	12*	13	0	25
	dlx3b/4b-MO	24	3	0	0	27
	b380	12	0	0	0	12
tbx1 (12 so)	*foxi1*$^{-/-}$	0	0	17	0	17
	dlx3b/4b-MO	19	4	0	0	23
	b380	12	0	0	0	12
neurog1 (24 hpf)	*dlx3b/4b*-MO	0	0	22	0	22
	b380	0	0	21	5	26
cdh10 (24 hpf)	*dlx3b/4b*-MO	0	4	19	0	23
	b380	5	14	0	0	19
tlx3b (24 hpf)	*dlx3b/4b*-MO	0	0	17	8	25
	b380	0	0	16	5	21
phox2a (24 hpf)	*dlx3b/4b*-MO	0	0	18	0	18
	b380	0	0	20	2	22
phox2bb (48 hpf)	*dlx3b/4b*-MO	0	0	19	0	19
	b380	0	0	18	0	18

*Only one sensory patch.

frequently, loss of Foxi1 reduces otic induction resulting in smaller *atoh1b* domains that do not separate into two domains during subsequent otic development.

Persistent OEPD-dependent neurogenesis in Dlx3b/4b- and Sox9a-deficient *b380* mutants

To corroborate our results, we analyzed a chromosome deficiency called *b380*, which lacks the genomic loci of *dlx3b*, *dlx4b* and *sox9a* physically and the OEPD expression of *pax2a* genetically (Fritz et al., 1996; Liu et al., 2003). Homozygous *b380* mutants completely lack otic placodes and fail to undergo otic vesicle morphogenesis, although a few residual cells, constituting an epithelial ball, express genes characteristic of the developing inner ear (Fritz et al., 1996; Liu et al., 2003). In contrast to Dlx3b/4b, Sox9a and Pax2a, which are all relevant to the second phase of the proposed otic induction model, expression of Foxi1 and Pax8, crucial for the first phase, are unaffected in *b380* mutants (Solomon and Fritz, 2002; Hans et al., 2004). At the onset of OEPD induction, *pax8* is strongly expressed but rapidly downregulated just prior to otic placode formation (Hans et al., 2004). However, persistence of DsRed protein in a gene trap in which the coding sequence of DsRed is inserted into the *pax8* locus (Ikenaga et al., 2011) allows us to track Pax8:DsRed-positive cells to later stages. To confirm the utility of this gene trap, we performed *in situ* hybridization with probes for *DsRed* and *pax8*. Compared with *pax8*, *pax8:DsRed* expression is elevated and more stable owing to the SV40 polyA signal contained in the gene trap vector, but the temporal and spatial patterns closely recapitulate endogenous *pax8* expression during otic development (supplementary material Fig. S3A-H). Live imaging of Pax8:DsRed-positive cells in wild-type embryos shows that OEPD Pax8-expressing cells give rise to the otic placode, which is morphologically visible at the 12-somite stage (Fig. 3A,E). Subsequently, Pax8:DsRed-positive cells label the entire otic vesicle and its associated neuroblasts, which have already delaminated by 24 hpf (Fig. 3C,G). By sharp contrast, Pax8:DsRed-positive cells are present but only loosely aggregated at the 12-somite or 24 hpf stages in *b380* mutants that do not show any morphological signs of otic placode or vesicle formation (Fig. 3B,D,F,H). Thus, OEPD Pax8-expressing cells are maintained after otic induction in *b380* mutants, and to examine their fates, we analyzed the expression of *neurod*, *cdh6*, *hmx3*, *myo7aa*, *atoh1b* and *tbx1*. As previously reported (Millimaki et al., 2007), *b380* mutants fail to form hair cells, demonstrated by the lack of *myo7aa* due to the loss of *atoh1b*, and they also lack otic *tbx1* expression in comparison with control siblings at 24 hpf or the 12-somite stage (Fig. 4M-R). By contrast, although no otic vesicle is formed, a large number of cells express *neurod* and *cdh6* in *b380* mutants (Fig. 4A,B,E,F). Furthermore, *neurod* expression within the otic vesicle, which is confined to an anterior-ventral position in control siblings, can be detected throughout the remaining epithelial ball in *b380* mutants (Fig. 4A,B). At the 12-somite stage, expression of *hmx3* can also be detected, although not

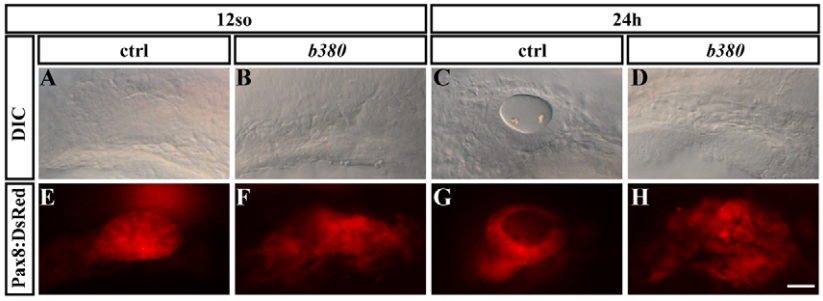

Fig. 3. Fate mapping of OEPD Pax8-expressing cells in wild-type and *b380* mutant embryos. (**A-H**) Live images of Pax8:DsRed in wild-type (A,C,E,G) and *b380* mutant (B,D,F,H) embryos at the 12-somite stage (A,B,E,F) and 24 hpf (C,D,G,H), respectively. Lateral views with anterior to the left. Scale bar: 40 μm.

in a discrete domain as in control siblings, but rather in a dispersed band of cells in *b380* mutants (Fig. 4I,J). To demonstrate that the underlying pathways leading to the expression of *neurod*, *cdh6* and *hmx3* are equivalent in control siblings and *b380* mutant embryos, we compromised the function of Neurog1 or Foxi1. We find that, similar to control embryos, loss of Neurog1 activity in *b380* mutant embryos completely abolishes *neurod* and *cdh6* but not *hmx3* expression at 24 hpf or 12-somite stages, respectively (Fig. 4C,G,K). Consistently, depletion of Foxi1 in *b380* mutant embryos results in the absence of *neurod*, *cdh6* and *hmx3* in the same manner as depletion of Foxi1 in control embryos at 24 hpf or the 12-somite stage (Fig. 4D,H,L). These results show that, in the absence of Dlx3b/4b and Sox9a, OEPD-dependent neurogenesis occurs and that the genetic pathways underlying OEPD-dependent neuronal development in *b380* mutants are identical to those in control embryos.

All neuronal OEPD derivatives are formed in Dlx3b/4b- and Sox9a-deficient *b380* mutants

Because previous studies have shown that the OEPD contributes to the statoacoustic, epibranchial and presumably anterior lateral line ganglia (McCarroll et al., 2012), we analyzed the identity of the neuronal progenitors in *b380* mutants. At 24 hpf, the proneural gene *neurogenin1* (*neurog1*) is expressed in a distinct pattern delineating the neurogenic placodes with strong expression in the progenitors of the anterior lateral line ganglion and in a subset of cells within the otic vesicle that will delaminate to form the statoacoustic ganglion (Andermann et al., 2002). In comparison with control or Dlx3b/4b-depleted embryos, *neurog1* is expressed in the progenitors of the anterior lateral line ganglion in *b380* mutants and a second strong expression domain is present despite the absence of the otic vesicle (Fig. 5A-C). To distinguish anterior lateral line and statoacoustic ganglion progenitors, we examined *T-cell leukemia, homeobox 3b* (*tlx3b*) and *cadherin10* (*cdh10*) expression (Langenau et al., 2002; Liu et al., 2006). Whereas *tlx3b* is exclusively expressed in trigeminal and anterior lateral line ganglion progenitors, as well as in the developing hindbrain (Langenau et al., 2002), *cdh10* is initially expressed in anterior lateral line ganglion progenitors, but is restricted to statoacoustic ganglion progenitors at 24 hpf (Liu et al., 2006). In *b380* mutants, expression of *cdh10* is reduced in comparison with control or Dlx3b/4b-depleted embryos at 24 hpf, whereas *tlx3b* appears increased in the absence of Dlx3b/4b as well

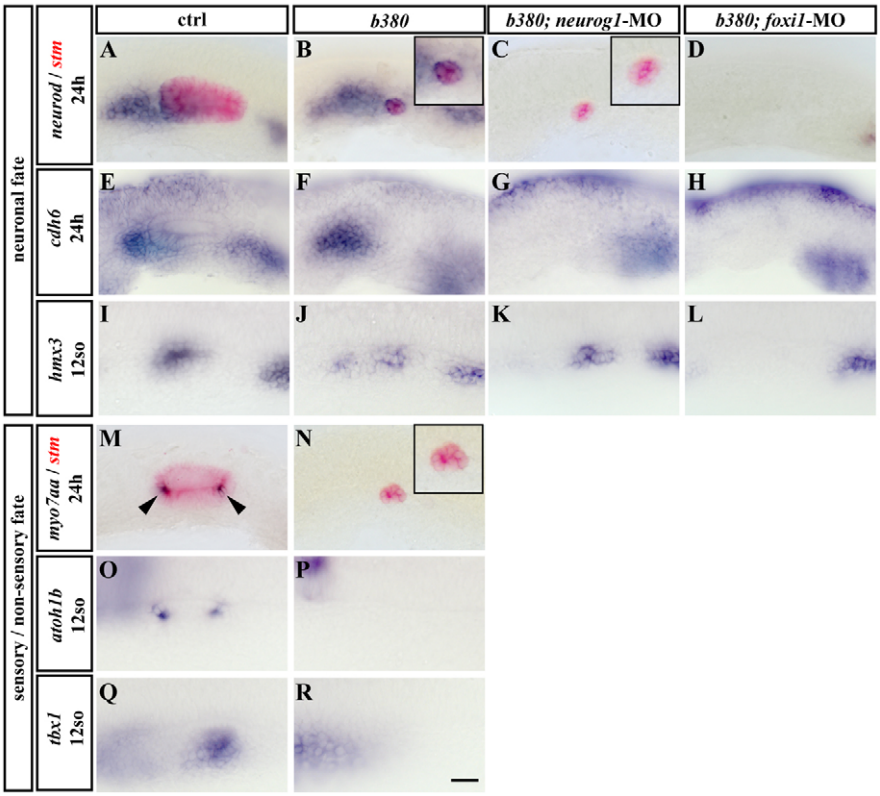

Fig. 4. Persistent OEPD-dependent neurogenesis in Dlx3b/4b- and Sox9a-deficient *b380* mutants. (**A-R**) Blue: Expression of *neurod* (A-D), *cdh6* (E-H), *hmx3* (I-L), *myo7aa* (M,N), *atoh1b* (O,P) and *tbx1* (Q,R) in control (A,E,I,M,O,Q), *b380* mutant (B,F,J,N,P,R), *b380*; *neurog1*-MO-injected (C,G,K) and *b380*; *foxi1*-MO-injected (D,H,L) embryos. Red: Expression of *stm* reveals the size of the otic vesicle which is reduced to a small epithelial ball in *b380* mutant and *b380*; *neurog1*-MO-injected and entirely absent in *b380; foxi1*-MO-injected embryos. A-H,M,N are lateral views with anterior to the left at 24 hpf. I-L,O,R are dorsolateral views with anterior to the left at the 12-somite stage. Insets in B, C and N show higher magnifications of the remaining otic tissue. Arrowheads in M indicate the position of the sensory patches. Scale bar: 40 μm.

as in *b380* mutants compared with control embryos at 24 hpf (Fig. 5D-I). To identify epibranchial ganglion progenitors, we examined the expression of *paired-like homeobox 2a* (*phox2a*) and *paired-like homeobox 2bb* (*phox2bb*) (Guo et al., 1999). At 24 hpf, expression of *phox2a* is initiated in the progenitors of the geniculate ganglion (gVII) in Dlx3b/4b-depleted embryos, *b380* mutants and control siblings (Fig. 5J-L). In comparison with control siblings at 48 hpf, *phox2bb* expression revealed that the petrosal (gIX) and nodose ganglion (gX) progenitors are also generated in a similar manner in the absence of Dlx3b/4b activity or in *b380* mutants (Fig. 5M-O). Taken together, our results show that all neuronal derivatives of the OEPD, the statoacoustic, anterior lateral line and epibranchial ganglia progenitors, are generated in the absence of Dlx3b/4b or in Dlx3b/4b- and Sox9a-deficient *b380* mutants.

DISCUSSION

Our results provide important insights into the acquisition of neuronal competence during inner ear development. In zebrafish, fate mapping of early OEPD cells using live imaging of a fluorescent reporter is challenging because endogenous *pax2a* expression is highly dynamic. The new conditional Cre recombination procedure we used here, PioTrack, importantly allows labeling of the first Cre-expressing cells of a nascent Cre domain owing to a conditional reporter that disconnects Cre-mediated recombination and reporter activation. The zebrafish temperature-inducible *hsp70l* promoter is inactive at normal temperatures and is only strongly and ubiquitously expressed during heat treatment (Halloran et al., 2000). Consequently, cells that have undergone recombination show reporter expression after heat treatment, and subsequent reporter persistence reveals the fate of these cells at later stages. By contrast, neighboring cells that initiate Cre expression after heat treatment undergo Cre-mediated recombination, but do not show reporter activity unless a second heat treatment is administered (Fig. 1). Furthermore, Cre-mediated recombination is a stochastic event, meaning that recombination does not happen in all Cre-expressing cells at the same time, and the probability of a recombination event increases as the concentration of Cre protein builds up over time (Nagy, 2000). Hence, our observation that EGFP-labeled cells are present throughout the otic vesicle only after heat treatment at placodal or later stages is due to delayed recombination and does not indicate that dorsal and posterior otic cells are added after otic placode formation. Using Kaede and caged fluorescein-dextran to label small groups of cells of the *pax2a*-positive OEPD showed that cells contributing to the otic vesicle are distributed throughout the *pax2a*-positive OEPD with some bias of anterolateral cells labeling the statoacoustic/anterior lateral line ganglia (McCarroll et al., 2012), which partly conflicts with our data. However, in our analysis, onset of *pax2a* expression regulated by Pax8 (Hans et al., 2004; Mackereth et al., 2005) correlates with the spatial distribution of labeled cells within the otic vesicle. Given that heterogeneous levels of Pax2a and Pax8 are found in the OEPD and high Pax2a and Pax8 levels correlate with otic fate (McCarroll et al., 2012), we assume that, in the Kaede and caged fluorescein-dextran approach, neighboring cells with differential Pax2a and Pax8 levels have been labeled that subsequently contribute to the entire otic vesicle. In this respect, our results are also consistent with the previous finding that high Pax2a and Pax8 levels correlate with otic fate (McCarroll et al., 2012), because early OEPD *pax2a*-positive cells always contribute to the anterior lateral line ganglia progenitors or otic lineage but never enter an epibranchial fate.

Previous studies in chick have shown that neural specification takes place only in the anterior region of the placode (Adam et al., 1998; Abelló et al., 2010), and our data indicate that the crucial determinative event occurs earlier, concurrent with OEPD induction. Previously the Foxi1-Pax8 pathway has been suggested to act as an early 'jumpstart' mediating the initial Fgf-dependent otic induction that occurs over a much shorter time period in zebrafish than in mice (Hans et al., 2004). We now show that in addition to otic induction, Foxi1 also provides competence to embark on a neuronal fate. Loss of Foxi1 results in a loss of *pax8* and in a patchy and variable onset of *pax2a* expression in the OEPD, which might explain why *foxi1* mutants develop small otic vesicles with no or just one otolith, whereas others have two small lumina each containing a single otolith (Nissen et al., 2003; Solomon et al., 2003). In contrast to this variable phenotype, compromised neurogenesis was robustly observed in all *foxi1* mutants examined (Table 1). Size reduction of the otic vesicle cannot alone explain this finding, because neurogenesis is not impaired in the absence of Dlx3b/4b activity, which causes a similar otic vesicle size reduction. Furthermore, other OEPD-derived neuronal derivatives, i.e. the progenitors of the anterior lateral line ganglion, are also absent in *foxi1* mutants. Taken together with previous findings showing that Foxi1 is required to specify OEPD-derived epibranchial progenitors (Lee et al., 2003), we propose that Foxi1 converts naive cells of the preplacodal region into the OEPD and provides neuronal competence for all OEPD-derived neuronal progenitors (Fig. 6). Expression analysis showed that at the end of gastrulation *foxi1* and *dlx3b*, a marker of the preplacodal region, share the same medial border, but *foxi1* extends further laterally (Solomon et al., 2003), supporting results that cells

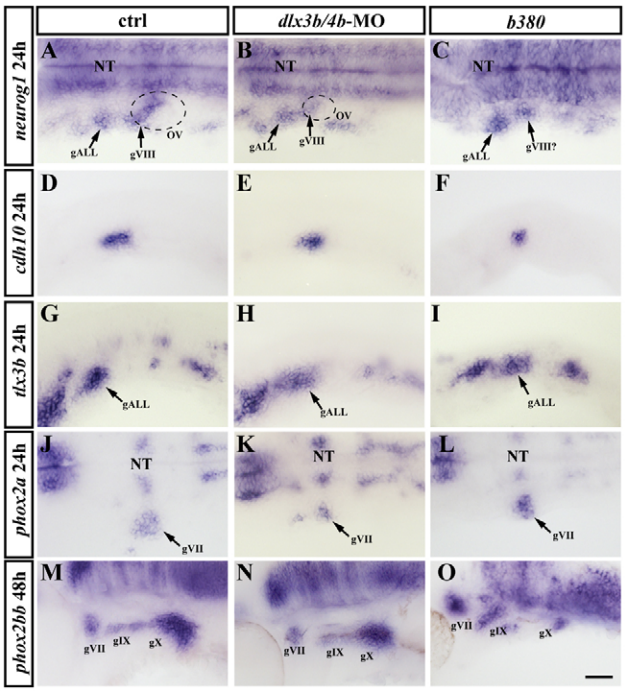

Fig. 5. All OEPD-derived neuronal progenitors are present in Dlx3b/4b-depleted embryos and Dlx3b/4b- and Sox9a-deficient *b380* mutants. (**A-O**) Expression of *neurog1* (A-C), *cdh10* (D-F), *tlx3b* (G-I), *phox2a* (J-L) and *phox2bb* (M-O) in control (A,D,G,J,M), Dlx3b/4b-depleted (B,E,H,K,N) and *b380* mutant embryos (C,F,I,L,O). A-C,J-L are dorsal views with anterior to the left at 24 hpf. D-I,M-O are lateral views with anterior to the left at 24 hpf (D-I) and 48 hpf (M-O). gVII, geniculate ganglion; gVIII, statoacoustic ganglion; gIX, petrosal ganglion; gX nodose ganglion; NT, neural tube; OV, otic vesicle. Scale bar: 50 μm.

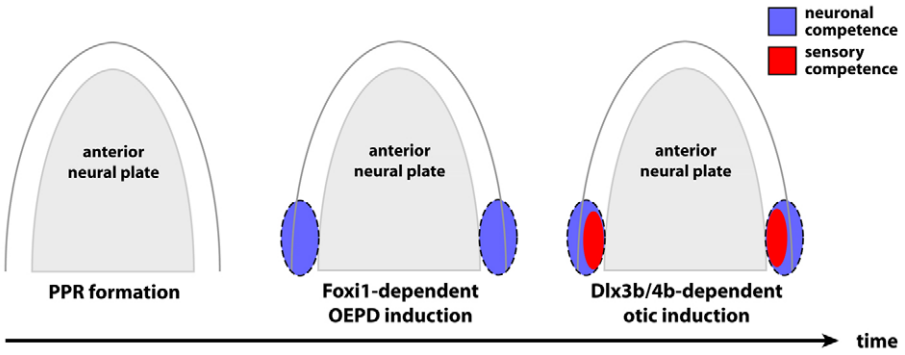

Fig. 6. Model of the early events providing competence to adopt a neuronal or sensory fate during inner ear development. After formation of the preplacodal region (PPR), Foxi1 initiates OEPD induction in the posterior PPR and further laterally provides competence to embark on a neuronal fate (blue). Subsequently, Dlx3b/4b, which is able to initiate otic induction in the absence of Foxi1, represses neuronal and imposes a sensory fate (red).

outside of the preplacodal region also contribute to epibranchial ganglia (Padanad and Riley, 2011; McCarroll et al., 2012). Subsequently, Dlx3b/4b, which is able to initiate otic induction in the absence of Foxi1, represses neuronal and imposes sensory fate by the activation of *atoh1b*. Consistently, it has been shown that neuronal differentiation is repressed after overexpression of Dlx3 (Pieper et al., 2012). However, although sensory hair cell formation is completely abolished and neuronal fate is increased in Dlx3b/4b-depleted embryos, nonsensory epithelial cells are still present and give rise to a size-reduced otic vesicle. This indicates that additional factors are required to repress Foxi1-mediated neuronal competence, and Sox9 is a likely candidate. Zebrafish *sox9a* and *sox9b* genes are duplicate orthologs of the human *SOX9* gene and both genes are expressed in the otic placode (Chiang et al., 2001). In *b380* mutants, *sox9a* is deleted and additional removal of Sox9b activity completely blocks all signs of otic specification and formation of the residual epithelial ball (Liu et al., 2003). It is unknown which OEPD-derived neuronal fate is still present in Sox9b-depleted *b380* mutants. We now show that all neuronal progenitors of the OEPD, the statoacoustic, anterior lateral line and epibranchial ganglia, are established in *b380* mutants. However, the number of statoacoustic ganglion progenitors is reduced whereas anterior lateral line progenitors are increased, indicating that in the absence of properly formed otic placode/vesicle, OEPD-derived cells embark on an anterior lateral line progenitor fate. Nevertheless, *neurod* expression within the otic vesicle, which is confined to an anterior-ventral position in wild-type embryos, is present throughout the remaining epithelial ball in *b380* mutants, showing that all otic cells adopt a neuronal fate in this genotype. Cell death as well as proliferation might also play an important role for proper neuronal progenitor formation, because Pax2 has been shown to play an important role in proliferation in the OEPD (Freter et al., 2012).

We also conclude that Foxi1 has no direct role in sensory hair cell formation, although absence of Foxi1 frequently results in smaller otic vesicles containing only one sensory patch. *foxi1* mutants display a highly variable otic phenotype that is foreshadowed by delayed and reduced expression of *pax2a* during OEPD induction (Nissen et al., 2003; Solomon et al., 2003). In wild-type embryos, sensory hair cell formation is initiated at OEPD stages highlighted by the expression of *atoh1b*, a proneural gene required for proper hair cell formation (Adolf et al., 2004; Millimaki et al., 2007). *atoh1b* expression is initiated prior to *pax2a* in a single prosensory domain that subsequently activates Delta-Notch feedback to split the domain into separate utricular and saccular primordia (Millimaki et al., 2007). In *foxi1* mutants, however, the initial single prosensory domain is frequently severely reduced in size and fails to subdivide into two separate domains.

It will be interesting to learn whether there is a similar developmental pattern in mammals. Mouse Foxi1 is expressed and required at a much later stage of inner ear development (Hulander et al., 2003), but expression of two other mouse Foxi family members, Foxi2 and Foxi3, coincide spatiotemporally with the period of otic induction. In particular, Foxi3 is expressed in a broad ectodermal region before and during otic induction and is subsequently downregulated in the developing placode similar to Foxi1 downregulation in zebrafish (Ohyama and Groves, 2004a). Thus, analysis of Foxi3 mutant mice will be necessary to learn whether this developmental pattern extends to mammals. Furthermore, how neuronal competence downstream of Foxi1 is executed remains elusive. The SoxB1 transcription factor Sox3 is expressed early in the OEPD region of chick and zebrafish and regulates the formation of the sensory-neural domain of the otic vesicle (Sun et al., 2007; Dee et al., 2008; Abelló et al., 2010). Furthermore, in zebrafish, Foxi1, but not Dlx3b/4b, is required for proper *sox3* expression, which is also unchanged in *b380* mutant embryos (Sun et al., 2007). Although a recent study reports no perceptible deficiency in neuronal precursor formation in the absence of Sox3 (Padanad and Riley, 2011), the finding that SoxB1 proteins control neural differentiation by directly regulating Neurog1 expression makes Sox3 a promising candidate (Okuda et al., 2010).

Acknowledgements
We thank Drs Q. Liu and M. Westerfield for sharing reagents; M. Fischer and J. Michling for excellent zebrafish care; the members of the Brand laboratory for discussions; and S. Linn and Dr M. Westerfield for comments on the manuscript.

Funding
This work was supported by the Deutsche Forschungsgemeinschaft [SFB655 and BR 1746/3-1]; the Technische Universität Dresden and the European Union (ZF-HEALTH – Zebrafish Regulomics for Human Health).

Competing interests statement
The authors declare no competing financial interests.

Supplementary material
Supplementary material available online at
http://dev.biologists.org/lookup/suppl/doi:10.1242/dev.087718/-/DC1

References
Abello, G. and Alsina, B. (2007). Establishment of a proneural field in the inner ear. *Int. J. Dev. Biol.* **51**, 483-493.
Abelló, G., Khatri, S., Radosevic, M., Scotting, P. J., Giráldez, F. and Alsina, B. (2010). Independent regulation of Sox3 and Lmx1b by FGF and BMP signaling influences the neurogenic and non-neurogenic domains in the chick otic placode. *Dev. Biol.* **339**, 166-178.
Adam, J., Myat, A., Le Roux, I., Eddison, M., Henrique, D., Ish-Horowicz, D. and Lewis, J. (1998). Cell fate choices and the expression of Notch, Delta and Serrate homologues in the chick inner ear: parallels with Drosophila sense-organ development. *Development* **125**, 4645-4654.

Adamska, M., Léger, S., Brand, M., Hadrys, T., Braun, T. and Bober, E. (2000). Inner ear and lateral line expression of a zebrafish Nkx5-1 gene and its downregulation in the ears of FGF8 mutant, ace. *Mech. Dev.* **97**, 161-165.
Adolf, B., Bellipanni, G., Huber, V. and Bally-Cuif, L. (2004). atoh1.2 and beta3.1 are two new bHLH-encoding genes expressed in selective precursor cells of the zebrafish anterior hindbrain. *Gene Expr. Patterns* **5**, 35-41.
Akimenko, M. A., Ekker, M., Wegner, J., Lin, W. and Westerfield, M. (1994). Combinatorial expression of three zebrafish genes related to distal-less: part of a homeobox gene code for the head. *J. Neurosci.* **14**, 3475-3486.
Alvarez, Y., Alonso, M. T., Vendrell, V., Zelarayan, L. C., Chamero, P., Theil, T., Bösl, M. R., Kato, S., Maconochie, M., Riethmacher, D. et al. (2003). Requirements for FGF3 and FGF10 during inner ear formation. *Development* **130**, 6329-6338.
Andermann, P., Ungos, J. and Raible, D. W. (2002). Neurogenin1 defines zebrafish cranial sensory ganglia precursors. *Dev. Biol.* **251**, 45-58.
Barald, K. F. and Kelley, M. W. (2004). From placode to polarization: new tunes in inner ear development. *Development* **131**, 4119-4130.
Bermingham, N. A., Hassan, B. A., Price, S. D., Vollrath, M. A., Ben-Arie, N., Eatock, R. A., Bellen, H. J., Lysakowski, A. and Zoghbi, H. Y. (1999). Math1: an essential gene for the generation of inner ear hair cells. *Science* **284**, 1837-1841.
Bouchard, M., de Caprona, D., Busslinger, M., Xu, P. and Fritzsch, B. (2010). Pax2 and Pax8 cooperate in mouse inner ear morphogenesis and innervation. *BMC Dev. Biol.* **10**, 89.
Brand, M., Heisenberg, C. P., Jiang, Y. J., Beuchle, D., Lun, K., Furutani-Seiki, M., Granato, M., Haffter, P., Hammerschmidt, M., Kane, D. A. et al. (1996). Mutations in zebrafish genes affecting the formation of the boundary between midbrain and hindbrain. *Development* **123**, 179-190.
Brand, M., Granato, M. and Nüsslein-Volhard, C. (2002). Keeping and raising zebrafish. In *Zebrafish, A Practical Approach*, pp. 7-37. Oxford: Oxford University Press.
Chen, J. and Streit, A. (2012). Induction of the inner ear: Stepwise specification of otic fate from multipotent progenitors. *Hear. Res.* **297**, 3-12.
Chiang, E. F. L., Pai, C.-I., Wyatt, M., Yan, Y.-L., Postlethwait, J. and Chung, B. (2001). Two sox9 genes on duplicated zebrafish chromosomes: expression of similar transcription activators in distinct sites. *Dev. Biol.* **231**, 149-163.
Dee, C. T., Hirst, C. S., Shih, Y.-H., Tripathi, V. B., Patient, R. K. and Scotting, P. J. (2008). Sox3 regulates both neural fate and differentiation in the zebrafish ectoderm. *Dev. Biol.* **320**, 289-301.
Ellies, D. L., Stock, D. W., Hatch, G., Giroux, G., Weiss, K. M. and Ekker, M. (1997). Relationship between the genomic organization and the overlapping embryonic expression patterns of the zebrafish dlx genes. *Genomics* **45**, 580-590.
Ernest, S., Rauch, G.-J., Haffter, P., Geisler, R., Petit, C. and Nicolson, T. (2000). Mariner is defective in myosin VIIA: a zebrafish model for human hereditary deafness. *Hum. Mol. Genet.* **9**, 2189-2196.
Freter, S., Muta, Y., Mak, S.-S., Rinkwitz, S. and Ladher, R. K. (2008). Progressive restriction of otic fate: the role of FGF and Wnt in resolving inner ear potential. *Development* **135**, 3415-3424.
Freter, S., Muta, Y., O'Neill, P., Vassilev, V. S., Kuraku, S. and Ladher, R. K. (2012). Pax2 modulates proliferation during specification of the otic and epibranchial placodes. *Dev. Dyn.* **241**, 1716-1728.
Fritz, A., Rozowski, M., Walker, C. and Westerfield, M. (1996). Identification of selected gamma-ray induced deficiencies in zebrafish using multiplex polymerase chain reaction. *Genetics* **144**, 1735-1745.
Fritzsch, B., Pauley, S. and Beisel, K. W. (2006). Cells, molecules and morphogenesis: the making of the vertebrate ear. *Brain Res.* **1091**, 151-171.
Fritzsch, B., Eberl, D. F. and Beisel, K. W. (2010). The role of bHLH genes in ear development and evolution: revisiting a 10-year-old hypothesis. *Cell. Mol. Life Sci.* **67**, 3089-3099.
Guo, S., Brush, J., Teraoka, H., Goddard, A., Wilson, S. W., Mullins, M. C. and Rosenthal, A. (1999). Development of noradrenergic neurons in the zebrafish hindbrain requires BMP, FGF8, and the homeodomain protein soulless/Phox2a. *Neuron* **24**, 555-566.
Haddon, C. and Lewis, J. (1996). Early ear development in the embryo of the zebrafish, Danio rerio. *J. Comp. Neurol.* **365**, 113-128.
Halloran, M. C., Sato-Maeda, M., Warren, J. T., Su, F., Lele, Z., Krone, P. H., Kuwada, J. Y. and Shoji, W. (2000). Laser-induced gene expression in specific cells of transgenic zebrafish. *Development* **127**, 1953-1960.
Hans, S., Liu, D. and Westerfield, M. (2004). Pax8 and Pax2a function synergistically in otic specification, downstream of the Foxi1 and Dlx3b transcription factors. *Development* **131**, 5091-5102.
Hans, S., Christison, J., Liu, D. and Westerfield, M. (2007). Fgf-dependent otic induction requires competence provided by Foxi1 and Dlx3b. *BMC Dev. Biol.* **7**, 5.
Hans, S., Kaslin, J., Freudenreich, D. and Brand, M. (2009). Temporally-controlled site-specific recombination in zebrafish. *PLoS ONE* **4**, e4640.
Hans, S., Freudenreich, D., Geffarth, M., Kaslin, J., Machate, A. and Brand, M. (2011). Generation of a non-leaky heat shock-inducible Cre line for conditional Cre/lox strategies in zebrafish. *Dev. Dyn.* **240**, 108-115.
Hulander, M., Kiernan, A. E., Blomqvist, S. R., Carlsson, P., Samuelsson, E.-J., Johansson, B. R., Steel, K. P. and Enerbäck, S. (2003). Lack of pendrin expression leads to deafness and expansion of the endolymphatic compartment in inner ears of Foxi1 null mutant mice. *Development* **130**, 2013-2025.
Ikenaga, T., Urban, J. M., Gebhart, N., Hatta, K., Kawakami, K. and Ono, F. (2011). Formation of the spinal network in zebrafish determined by domain-specific pax genes. *J. Comp. Neurol.* **519**, 1562-1579.
Kimmel, C. B., Ballard, W. W., Kimmel, S. R., Ullmann, B. and Schilling, T. F. (1995). Stages of embryonic development of the zebrafish. *Dev. Dyn.* **203**, 253-310.
Krauss, S., Johansen, T., Korzh, V. and Fjose, A. (1991). Expression of the zebrafish paired box gene pax[zf-b] during early neurogenesis. *Development* **113**, 1193-1206.
Kroehne, V., Freudenreich, D., Hans, S., Kaslin, J. and Brand, M. (2011). Regeneration of the adult zebrafish brain from neurogenic radial glia-type progenitors. *Development* **138**, 4831-4841.
Ladher, R. K., Wright, T. J., Moon, A. M., Mansour, S. L. and Schoenwolf, G. C. (2005). FGF8 initiates inner ear induction in chick and mouse. *Genes Dev.* **19**, 603-613.
Ladher, R. K., O'Neill, P. and Begbie, J. (2010). From shared lineage to distinct functions: the development of the inner ear and epibranchial placodes. *Development* **137**, 1777-1785.
Langenau, D. M., Palomero, T., Kanki, J. P., Ferrando, A. A., Zhou, Y., Zon, L. I. and Look, A. T. (2002). Molecular cloning and developmental expression of Tlx (Hox11) genes in zebrafish (Danio rerio). *Mech. Dev.* **117**, 243-248.
Lee, S. A., Shen, E. L., Fiser, A., Sali, A. and Guo, S. (2003). The zebrafish forkhead transcription factor Foxi1 specifies epibranchial placode-derived sensory neurons. *Development* **130**, 2669-2679.
Léger, S. and Brand, M. (2002). Fgf8 and Fgf3 are required for zebrafish ear placode induction, maintenance and inner ear patterning. *Mech. Dev.* **119**, 91-108.
Liu, D., Chu, H., Maves, L., Yan, Y.-L., Morcos, P. A., Postlethwait, J. H. and Westerfield, M. (2003). Fgf3 and Fgf8 dependent and independent transcription factors are required for otic placode specification. *Development* **130**, 2213-2224.
Liu, Q., Duff, R. J., Liu, B., Wilson, A. L., Babb-Clendenon, S. G., Francl, J. and Marrs, J. A. (2006). Expression of cadherin10, a type II classic cadherin gene, in the nervous system of the embryonic zebrafish. *Gene Expr. Patterns* **6**, 703-710.
Ma, Q., Chen, Z., del Barco Barrantes, I., de la Pompa, J. L. and Anderson, D. J. (1998). neurogenin1 is essential for the determination of neuronal precursors for proximal cranial sensory ganglia. *Neuron* **20**, 469-482.
Mackereth, M. D., Kwak, S.-J., Fritz, A. and Riley, B. B. (2005). Zebrafish pax8 is required for otic placode induction and plays a redundant role with Pax2 genes in the maintenance of the otic placode. *Development* **132**, 371-382.
Maroon, H., Walshe, J., Mahmood, R., Kiefer, P., Dickson, C. and Mason, I. (2002). Fgf3 and Fgf8 are required together for formation of the otic placode and vesicle. *Development* **129**, 2099-2108.
McCarroll, M. N., Lewis, Z. R., Culbertson, M. D., Martin, B. L., Kimelman, D. and Nechiporuk, A. V. (2012). Graded levels of Pax2a and Pax8 regulate cell differentiation during sensory placode formation. *Development* **139**, 2740-2750.
Millimaki, B. B., Sweet, E. M., Dhason, M. S. and Riley, B. B. (2007). Zebrafish atoh1 genes: classic proneural activity in the inner ear and regulation by Fgf and Notch. *Development* **134**, 295-305.
Nagy, A. (2000). Cre recombinase: the universal reagent for genome tailoring. *Genesis* **26**, 99-109.
Nissen, R. M., Yan, J., Amsterdam, A., Hopkins, N. and Burgess, S. M. (2003). Zebrafish foxi one modulates cellular responses to Fgf signaling required for the integrity of ear and jaw patterning. *Development* **130**, 2543-2554.
Ohyama, T. and Groves, A. K. (2004a). Expression of mouse Foxi class genes in early craniofacial development. *Dev. Dyn.* **231**, 640-646.
Ohyama, T. and Groves, A. K. (2004b) Generation of Pax2-Cre mice by modification of a Pax2 bacterial artificial chromosome. *Genesis* **38**, 195-199.
Okuda, Y., Ogura, E., Kondoh, H. and Kamachi, Y. (2010). B1 SOX coordinate cell specification with patterning and morphogenesis in the early zebrafish embryo. *PLoS Genet.* **6**, e1000936.
Padanad, M. S. and Riley, B. B. (2011). Pax2/8 proteins coordinate sequential induction of otic and epibranchial placodes through differential regulation of foxi1, sox3 and fgf24. *Dev. Biol.* **351**, 90-98.
Pfeffer, P. L., Gerster, T., Lun, K., Brand, M. and Busslinger, M. (1998). Characterization of three novel members of the zebrafish Pax2/5/8 family: dependency of Pax5 and Pax8 expression on the Pax2.1 (noi) function. *Development* **125**, 3063-3074.
Phillips, B. T., Bolding, K. and Riley, B. B. (2001). Zebrafish fgf3 and fgf8 encode redundant functions required for otic placode induction. *Dev. Biol.* **235**, 351-365.
Picker, A., Scholpp, S., Böhli, H., Takeda, H. and Brand, M. (2002). A novel positive transcriptional feedback loop in midbrain-hindbrain boundary

development is revealed through analysis of the zebrafish pax2.1 promoter in transgenic lines. *Development* **129**, 3227-3239.
Pieper, M., Ahrens, K., Rink, E., Peter, A. and Schlosser, G. (2012). Differential distribution of competence for panplacodal and neural crest induction to non-neural and neural ectoderm. *Development* **139**, 1175-1187.
Piotrowski, T., Ahn, D. G., Schilling, T. F., Nair, S., Ruvinsky, I., Geisler, R., Rauch, G.-J., Haffter, P., Zon, L. I., Zhou, Y. et al. (2003). The zebrafish van gogh mutation disrupts tbx1, which is involved in the DiGeorge deletion syndrome in humans. *Development* **130**, 5043-5052.
Radosevic, M., Robert-Moreno, À., Coolen, M., Bally-Cuif, L. and Alsina, B. (2011). Her9 represses neurogenic fate downstream of Tbx1 and retinoic acid signaling in the inner ear. *Development* **138**, 397-408.
Rubel, E. W. and Fritzsch, B. (2002). Auditory system development: primary auditory neurons and their targets. *Annu. Rev. Neurosci.* **25**, 51-101.
Sapède, D., Dyballa, S. and Pujades, C. (2012). Cell lineage analysis reveals three different progenitor pools for neurosensory elements in the otic vesicle. *J. Neurosci.* **32**, 16424-16434.
Satoh, T. and Fekete, D. M. (2005). Clonal analysis of the relationships between mechanosensory cells and the neurons that innervate them in the chicken ear. *Development* **132**, 1687-1697.
Söllner, C., Burghammer, M., Busch-Nentwich, E., Berger, J., Schwarz, H., Riekel, C. and Nicolson, T. (2003). Control of crystal size and lattice formation by starmaker in otolith biomineralization. *Science* **302**, 282-286.
Solomon, K. S. and Fritz, A. (2002). Concerted action of two dlx paralogs in sensory placode formation. *Development* **129**, 3127-3136.
Solomon, K. S., Kudoh, T., Dawid, I. B. and Fritz, A. (2003). Zebrafish foxi1 mediates otic placode formation and jaw development. *Development* **130**, 929-940.
Solomon, K. S., Kwak, S.-J. and Fritz, A. (2004). Genetic interactions underlying otic placode induction and formation. *Dev. Dyn.* **230**, 419-433.
Streit, A. (2007). The preplacodal region: an ectodermal domain with multipotential progenitors that contribute to sense organs and cranial sensory ganglia. *Int. J. Dev. Biol.* **51**, 447-461.
Sun, S.-K., Dee, C. T., Tripathi, V. B., Rengifo, A., Hirst, C. S. and Scotting, P. J. (2007). Epibranchial and otic placodes are induced by a common Fgf signal, but their subsequent development is independent. *Dev. Biol.* **303**, 675-686.
Westerfield, M. (2000). *The Zebrafish Book: A Guide for the Laboratory Use of Zebrafish (Danio rerio)*, 4th edn. Eugene, OR: University of Oregon Press.
Wright, T. J. and Mansour, S. L. (2003). Fgf3 and Fgf10 are required for mouse otic placode induction. *Development* **130**, 3379-3390.

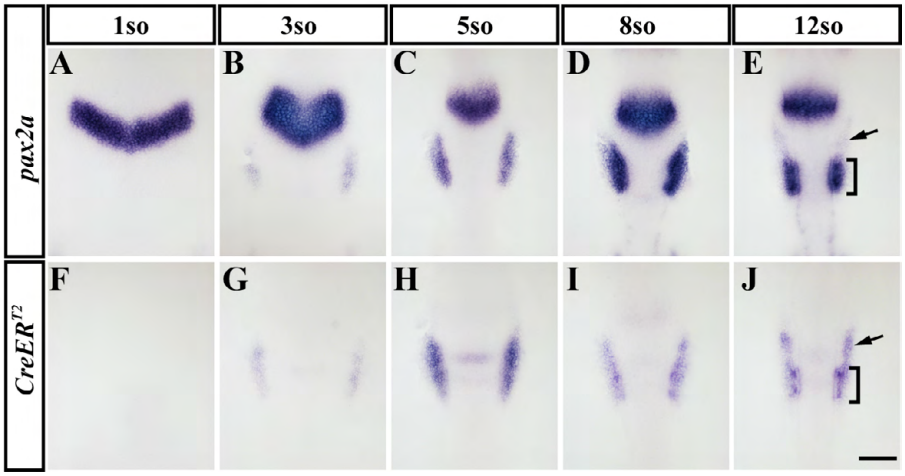

Fig. S1. Expression of *CreER^{T2}* recapitulates the endogenous *pax2a* expression during OEPD development. (**A-J**) The temporal and spatial expression of *CreER^{T2}* (F-I) within the OEPD is identical to *pax2a* (A-D) in *Tg(pax2a:CreER^{T2})$^{\#31}$* transgenic embryos. Subsequently, *pax2a* (E) is maintained exclusively in the otic placode (bracket) but is downregulated in non-incorporated cells anteriorly to it (arrow), whereas *CreER^{T2}* (J) is sustained in both regions. Dorsal views with anterior to the top at the 1-, 3-, 5-, 8- and 12-somite (so) stages, as indicated. Scale bar: 100 µm.

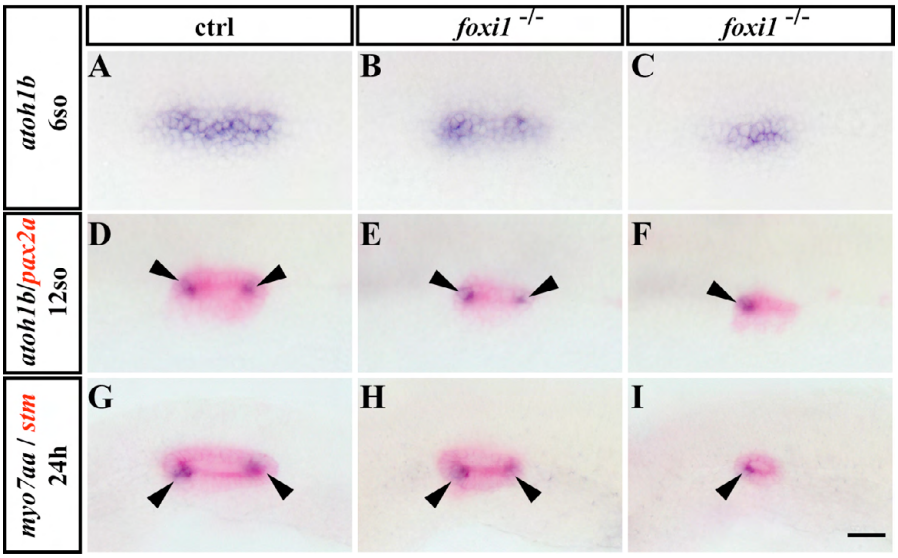

Fig. S2. Hair cell formation is highly variably in *foxi1* mutants, which is foreshadowed by *atoh1b* expression at OEPD stages. (**A-I**) Blue: Expression of *atoh1b* (A-F) and *myo7aa* (G-I) in control (A,D,G) and *foxi1* mutant embryos (B,C,E,F,H,I). Red: Expression of *pax2a* and *stm* reveal size of the otic placode and vesicle, respectively. A-C are dorsal views with anterior to the top at the 3-somite stage. D-F are dorsolateral views with anterior to the left at the 12-somite stage. G-I are lateral views with anterior to the left at 24 hpf. Arrowheads indicate the position of the sensory patches. Scale bar: 35 µm.

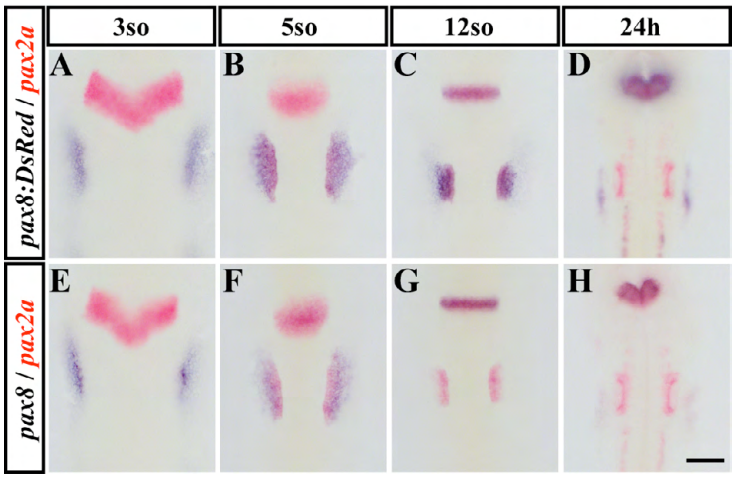

Fig. S3. Expression of *DsRed* in a gene trap in which the coding sequence of DsRed is inserted into the *pax8* locus, recapitulates the endogenous *pax8* expression during otic development. (**A-H**) Blue: Expression of *DsRed* (A-D) and *pax8* (E-H) in *pax8*^{nia03Gt} transgenic embryos. Red: Expression of *pax2a*. Dorsal views with anterior to the top at the 3-, 5-, 12-somite (so) stage and 24 hpf, as indicated. Scale bar: 100 µm.